Preprint
UCRL-CR-139054

Demonstration of Pu Immobilisation in Synroc at the 50g of PuO_2 Scale

S. Moricca, A. J. Brownscombe, N. Webb, M. W. A. Stewart, R. A. Day, M. Hambley, E. R. Vance and A. Jostsons

U.S. Department of Energy

Lawrence
Livermore
National
Laboratory

June 1, 1997

This work was performed under the auspices of the U.S. Department of Energy by University of California, Lawrence Livermore National Laboratory under Contract W-7405-Eng-48.

ANSTO Report/C511

Demonstration of Pu Immobilisation in Synroc at the 50g of PuO_2 Scale

S. Moricca, A.J. Brownscombe, N. Webb, M.W.A. Stewart,
R.A. Day, M. Hambley, E. R. Vance and A. Jostsons

Materials Division, ANSTO
PMB 1 Menai, NSW, 2234
Australia

June 1997

Demonstration of Pu Immobilisation in Synroc at the 50g of PuO_2 Scale

S. Moricca, A.J. Brownscombe, N. Webb, M.W.A. Stewart,
R.A. Day, M. Hambley, E. R. Vance and A. Jostsons

Materials Division, ANSTO
PMB 1 Menai, NSW, 2234
Australia

Summary

The immobilisation of 13.5 wt% PuO_2 in a zirconolite-rich Synroc has been demonstrated at the 50 g PuO_2 scale in cans produced by hot isostatic pressing (HIPing) at 1280°C. The wasteform also contains more than an equimolar amount of neutron poisons such as Gd, Sm and Hf. The scale-up of technology for production of Pu-containing cans of Synroc by HIPing has been demonstrated at the 10 kg scale using CeO_2 as an analog for PuO_2. The characterisation of the products has shown that Ce is a good analog for Pu in zirconolite-rich Synroc produced by HIPing. Post-production thermal tests simulating the effects of a HLW glass pour in a surrounding canister have shown that the Synroc is stable and there is no exsolution of PuO_2 or CeO_2. The report contains results of characterisation to complete the terms of the Subcontract B33691 to ANSTO from the Regents of the University of California, USA, with Lawrence Livermore National Laboratory as the Prime Contractor to the U.S. DOE under Contract W-7405-ENG-48.

INTRODUCTION

Immobilisation in glass or ceramic waste forms remains one of the alternatives preferred by the U.S. DOE for the disposition of surplus weapons plutonium. To capitalise on the existing infrastructure at U.S. DOE sites, the can-in-canister option has been highlighted by the DOE for this purpose. The work described in this report was designed to demonstrate, using ANSTO proprietary technology on Synroc, that:

- ceramic wasteforms based on Synroc can immobilise high Pu loadings in solid solution together with a range of neutron poisons;
- technology exists that can be credibly demonstrated up to production scale.

The demonstration involved a zirconolite-rich Synroc containing more than 50gm of PuO_2 (including minor in-grown Am_2O_3). The Synroc was produced by hot isostatic pressing (HIPing) in metal cans. The nominal phase composition (wt.%) of the zirconolite-rich Synroc was 80% zirconolite, 10% hollandite and 10% rutile. The nominal loading of PuO_2, neutron poisons and Ga_2O_3 in the zirconolite-rich Synroc was:

PuO_2 - 13.5 ± 1.0 wt.%
HfO_2 - 10 ± 1 wt.%
Gd_2O_3 - 4 ± 1 wt.%
Sm_2O_3 - 4 ± 1 wt.%
Ga_2O_3 - 0.15 ± 0.05 wt.%

The demonstration was performed by ANSTO under subcontract B33691 from The Regents of the University of California, U.S.A., with Lawrence Livermore National Laboratory (LLNL) as the Prime Contractors to the U.S. DOE under Contract W-7405-ENG-48.

The demonstration contract required the production of duplicate cans of Synroc with PuO_2 and with rare earth simulants of PuO_2. One set of cans was to be shipped to LLNL; the other to be characterised by ANSTO. The tasks are set out below:

Item 1	PuO_2 immobilisation in Synroc on a 50gm scale as per the composition listed above.
Item 2	Can similar to Item 1 with PuO_2 substituted by CeO_2 on a molar basis.
Item 3	Zirconolite-rich Synroc in cans containing 10 ± 1 kg of Synroc ceramic with CeO_2 substituted for PuO_2 on a molar basis to demonstrate can production scale-up.

2. METHODS

2.1 Processing

The Synroc precursor, including all neutron poisons, was produced by the ANSTO standard alkoxide hydrolysis route. PuO_2 was dissolved in 16M HNO_3, blended with the precursor, and the mixture was calcined for 1 hour at 750°C in argon. The calcined powder was then ball milled, dried and loaded into cans for HIPing. The HIP cans were then evacuated to 50 mtorr during heating to 800^0C to drive off residual water and welded shut. These steps were carried out in ANSTO's glove box facility. The plutonium isotopic content, determined by γ spectroscopy of a dilute solution with a germanium well detector, was found to be Pu239: Pu240 : Pu241 : Am241 in the ratio 93 : 5 : 0 .45 : 1.55.

The simulation, Item 2, was performed by substituting CeO_2 for PuO_2 in Item 1 on a molar basis. The preparation of the powder and cans of the CeO_2 simulated Synroc was identical to that of the PuO_2 Synroc, with the exception that the 'waste' was added as a cerium nitrate solution.

The powder for the scale-up Item 3, was not milled after calcination as for Items 1 and 2. In this large batch, Sm was largely replaced on a molar basis by Gd, and Hf by Zr.

The sealed cans for items 1 and 2 were HIPed at 1270-1280^0C for 2 hours. The 10 kg batch, Item 3 was HIPed at 1240^0C.

Table 1. Target composition of zirconolites (~ Ca $ZrTi_2O_7$)

Item	Ca	Pu	Ce	Gd	Sm	Hf	Zr	Ti	Al	O
1	0.595	0.27		0.135	0.135	0.27	0.595	1.73	0.27	7
2	0.595	-	0.27	0.135	0.135	0.27	0.595	1.73	0.27	7
3	0.595	-	0.27	0.25	0.02	0.005	0.86	1.73	0.27	7

2.2 Characterisation

Cores, 10mm dia., were extracted from the HIPed cans and slices were cut from the cores and metallographically polished for examination. A JEOL 6300 SEM fitted with a NORAN 'Voyager' energy dispersive x-ray analysis system and a Pioneer low-element detector was used for microstructural characterisation and micro-analysis. Quantitative image analysis was employed to determine volume fractions of phases and closed porosity. The phase weight fractions were derived from the volume fractions by appropriate weighting for densities derived from unit cell measurements and determinations of phase elemental contents.

For x-ray diffraction, the PuO_2 containing specimens were mounted in epoxy resin, polished and examined on a SCINTAG 'X1' diffractometer with Cu Kα radiation. The cerium analog specimens after crushing were also examined on a Siemens 'Kristalloflex' instrument using Co Kα radiation.

Bulk densities of specimens were determined by immersion techniques.

Standard MCC-1 type leaching tests have commenced. Preliminary results from a 0-7 day MCC-1 leach test at 70^0C in deionised water show a normalised Pu leach rate of $3\text{-}5\times10^{-6}$ $g.m^{-2}.d^{-1}$ from unfiltered solutions, i.e. Pu in solution and as colloids.

3. RESULTS

3.1 Structural Characterisation

The microstructures of the PuO_2 containing Synroc (Item 1) and its CeO_2 analog (Item 2) are shown in Figures 1 and 2 respectively. The x-ray diffraction patterns are shown in Figure 3. In both cases the desired phase assemblage has been obtained (Table 2) and the specimens are homogeneous on a 10μm scale. The phase compositions and contents are given in Table 2 and Table 3 lists additional parameters that show that high density has been achieved and the resultant grain size is small. The microanalytical results for hollandite and rutile are approximate since very few grains were big enough to ensure that x-ray scattering from neighbouring phases was fully excluded.

The lattice parameters of zirconolite in the Ce analog and Pu specimens were determined to correct the vol.% phase content to weight%. The lattice parameters are listed below:

Lattice parameters of zirconolite (^{0}A) and deg. (Monoclinic angle)

	a	b	c	β
Pu-doped	12.5367_5	7.2381_3	11.2945_5	100.661_1
Ce-doped	12.5491_4	7.2452_2	11.3027_3	100.664_1

Lattice parameters of hollandite and rutile phases

	a_H	c_H	a_R	c_R
Pu-doped	10.010_5	*	4.6020_3	2.9758_6
Ce-doped	9.9759_4	2.9269_2	4.6034_2	2.9746_1

* only the 310 line could be identified so it is not possible to evaluate c_H

TABLE 2 : Phase Composition of Material from HIP cans.

TABLE 2a : Pu bearing SYNROC

PHASE	AVERAGE PHASE COMPOSITION	Vol. %	Wt. %
Zirconolite	$Ca_{0.54}Sm_{0.11}Gd_{0.11}Pu_{0.32}Hf_{0.26}Zr_{0.48}Ti_{1.73}Al_{0.34}O_7$	73	79
Hollandite	$Ba_{1.03}Al_{1.59}Cr_{0.22}Ti_{6.12}O_{16}$ *	16	12
Rutile	TiO_2 with ~ 6wt% Hf and 4 wt% Zr	10	8
Porosity		1	1

TABLE 2b : Ce analog

PHASE	AVERAGE PHASE COMPOSITION	Vol. %	Wt. %
Zirconolite	$Ca_{0.50}Sm_{0.13}Gd_{0.12}Ce_{0.27}Hf_{0.25}Zr_{0.43}Ti_{1.86}Al_{0.36}O_7$	75	80
Hollandite	$Ba_{1.09}Al_{2.06}Ti_{6.00}O_{16}$ #	14	12
Rutile	TiO_2 (particles too small to determine presence of Zr or Hf)	10	8
Porosity		<0.1	-

* Cr was picked up from stainless steel vessels during processing.
# Grain sizes were on the limit for accurate analysis (≈ 1μm)

TABLE 3 : Characteristics of the HIPed Material

	Pu BEARING SYNROC	Ce ANALOG
Density (g/cm^3)	~ 5.1	~ 5.0
Surface Porosity (vol%)	~ 0.1%	~ 0.1%
Closed Porosity (vol%)	~ 1%	< 0.1%
Grain size (μm)	1-4	1-2

The normal (500 second) EDS analysis of phases did not identify gallium which was introduced at the 0.15 wt.% level in the batches of items 1 and 2. Subsequent (5000 second) searches for trace amounts of gallium in the Synroc phases revealed the presence of gallium L line peaks from spectra collected from hollandite and from zirconolite but not from rutile. On the basis of the observed Ga peak it appears that the Ga concentration is somewhat higher in the hollandite than the zirconolite. This deduction takes into account the need to make an allowance for interference from the Sm M lines from zirconolite.

The microstructure of the large batch (Item 3), Figure 3, was not as homogeneous as the cerium analog material (Item 2) because a milling step was deliberately omitted since the aim of Item 3 was primarily to demonstrate HIP can scale-up. In a production plant, rabble bars in rotary calciners avoid the formation of agglomerates. In the present work a simple laboratory tube furnace was used for calcination. The higher magnification microstructures (Figs.4(b) and 4(c)) nevertheless revealed interesting features:

- occurrence of possible CeO_2 particles that would imply that local solubility limits have been exceeded;
- occurrence of pyrochlore as an additional phase (4c). The small cerium oxide particles noted above may well be pyrochlore but they are too small for definitive identification by EDS on the SEM.

Neither of the above two phases could be identified by powder x-ray diffraction methods.

3.2 Post processing heat treatment

The can-in-canister concept envisages that the cans of Pu containing waste form would be loaded into a canister in which HLW glass would be poured subsequently. We have briefly investigated the possible effects of post processing heat treatment on the microstructure of the Synroc. The thermal regime upon contact with molten DWPF glass was simulated by reheating specimens of Synroc to 1100^0C in an argon atmosphere followed by controlled cooling at 0.5^0C/min to 900^0C and then furnace cooling (~ 5^0C/min) to ambient. Such tests on the Pu specimen (Item 1) and Ce analog (Item 2) did not lead to any significant change in microstructure as shown in Figs.5(a) and (b). Specifically, PuO_2 nor CeO_2 exsolved from Synroc phases under this simulated thermal treatment.

3.3 HIPed cans

The HIPed cans of zirconolite-rich Synroc for items 2 and 3 are shown in Figure 6. These have been sent to LLNL as per contract. The Pu containing can (Item 1) Fig.7 is stored at ANSTO awaiting decisions from LLNL on shipment. The characterisation described previously has been performed on specimens from duplicate cans of Items 1-3.

The main parameters of the cans are shown below:

	Synroc content (gm)	Approximate	
		diameter	height (mm)
Item 1	366	62	41
Item 2	256	62	36.5
Item 3	9510	121	240

These parameters satisfy fully the terms of the contract. It is noted (see below) that the PuO_2 content is higher than the nominal 13.5 wt.% and hence the can in Item 1 contains more than 50gm of immobilised PuO_2.

The powder for Item 2 had a lower packing density than expected. Consequently, ANSTO has manufactured a larger amount of the Ce analog material in a 'double' bellows configuration as shown in Fig.7. This demonstrates an intermediate step in the ANSTO proprietary HIP bellows design. At the same time the additional can of Item 2 is intended to provide LLNL with extra material for independent characterisation of the non-radioactive simulation of Pu immobilisation in Synroc.

4. DISCUSSION

The demonstration has achieved both aims and some additional items have been supplied on the thermal stability of the Ce simulated zirconolite-rich Synroc. The PuO_2 content immobilised in the Synroc was at the higher end of the specified range. As shown in Table 2a the zirconolite average composition (in one formula unit) corresponded to $Pu_{O..32}$ instead of the nominal value of $Pu_{O..27}$, Table 1.

One measure to increase the Pu content of zirconolite-rich Synroc would be to decrease the amounts of hollandite and excess rutile. However, ANSTO strongly believes that there are benefits in maintaining a multi-phase formulation for process flexibility and to minimise grain growth. Small grain size is desirable to enhance resistance to radiation damage effects.

Another avenue of increasing Pu loadings in zirconolite-rich Synroc is to reconsider the loading of neutron poisons. Full replacement of Zr by Hf may permit elimination of Gd or Sm. Gd and Sm compete for the same sites as Pu in zirconolite. The elimination of one of them would permit 50% higher Pu loadings, i.e. about 20wt.% PuO_2, without a need to change the phase ratios. Still higher loadings of Pu are possible if the waste formulation is changed to encourage formation of zirconolite II and/or pyrochlore.

The microstructures of the Pu and Ce formulation together with the phase compositions shown in Table 2 clearly demonstrate that Ce is an effective analog for Pu in zirconolite-rich Synroc processed under the conditions employed in this demonstration, i.e. HIPing in evacuated cans.

The HIP cans sent to LLNL (Items 2 and 3) demonstrate the technology developed previously at ANSTO to produce Synroc monoliths of near theoretical density. Cans containing more than 30kg of Synroc-C have been produced at ANSTO at 1200^0C. Large variations in the diameter versus length of the HIP cans are possible to meet the requirements of the can-in-canister concept for Pu immobilisation.

5. CONCLUSIONS

1. The immobilisation of PuO_2 in a zirconolite-rich Synroc has been demonstrated at the 50gm PuO_2 scale. The waste form contains simultaneously more than an equimolar amount of neutron poisons such as Gd, Sm and Hf.
2. Ce is a good analog for Pu in zirconolite-rich Synroc produced by HIPing.
3. The Pu Synroc and the Ce analog in post-production thermal tests simulating effects on zirconolite-rich Synroc from a HLW glass pour in the canister demonstrate stability against phase alteration and exsolution PuO_2 and CeO_2.
4. The HIPing technology of Synroc has been demonstrated at near production scale for the can-in-canister concept for PuO_2 immobilisation.

ACKNOWLEDGMENTS

The financial support of the U.S. DOE through Lawrence Livermore National Laboratory for the demonstration of ANSTO's proprietary technology is acknowledged as is the continuing support of the Australian Government that has been essential for the development of these technologies.

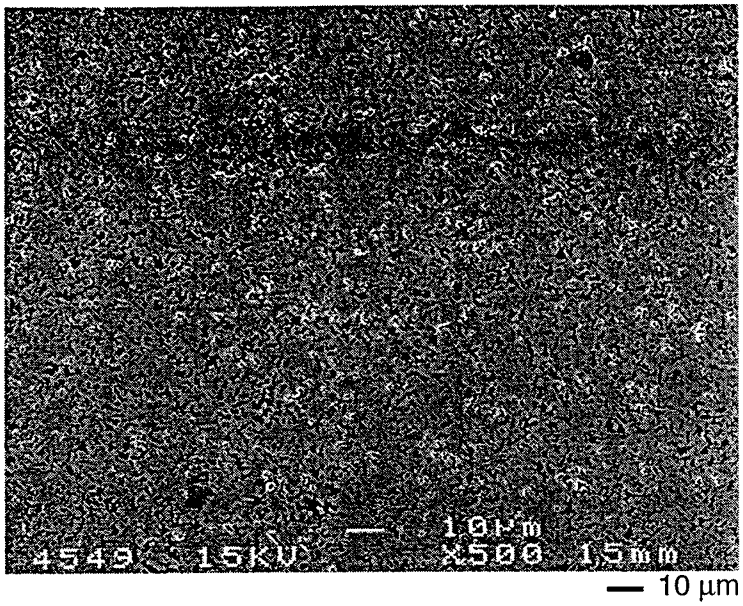

Figure 1a

Secondary electron image showing porosity (distinguished by bright borders), mainly at triple points, evenly distributed throughout the Pu SYNROC. (500x)

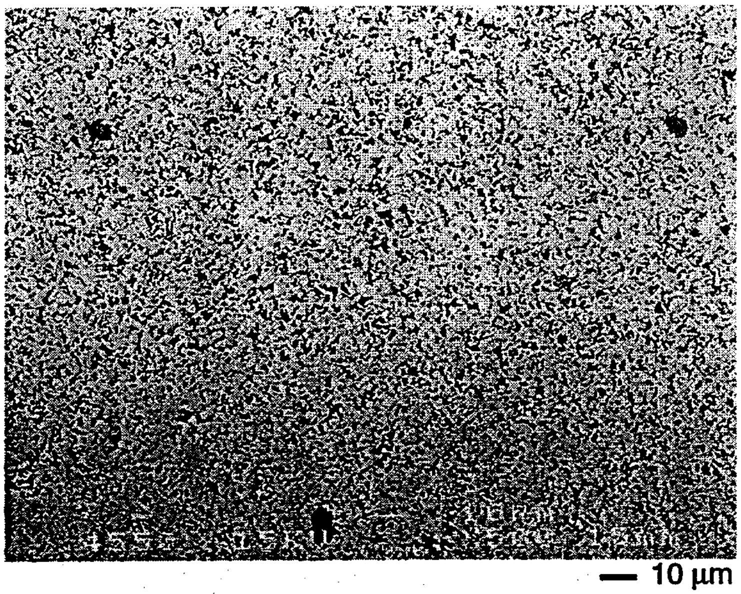

Figure 1b

Backscattered electron image showing homogeneity of the Pu SYNROC. (500x)

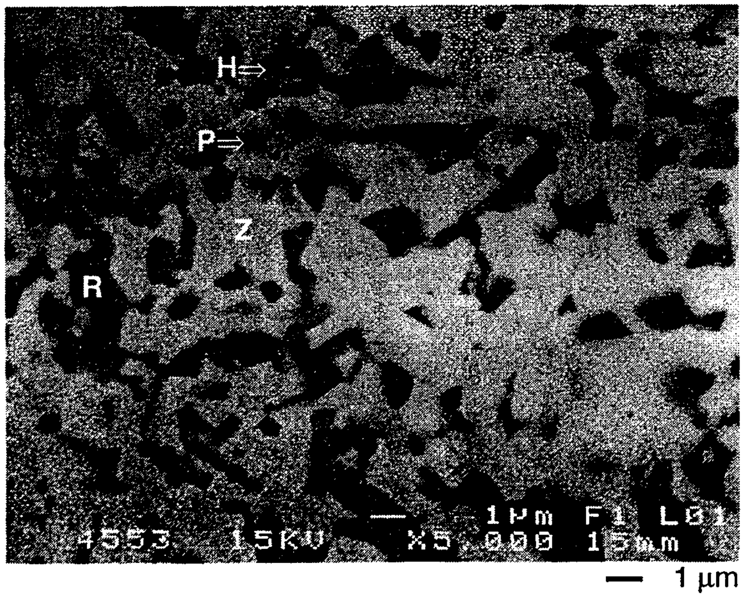

Figure 1c

Backscattered electron image showing detail of the phases present in the Pu SYNROC. (5000x) Z = Zirconolite, H = Hollandite, R = Rutile,P = Pores

FIGURE 1 : SEM Images of the Pu SYNROC Material HIPed at 1280°C.

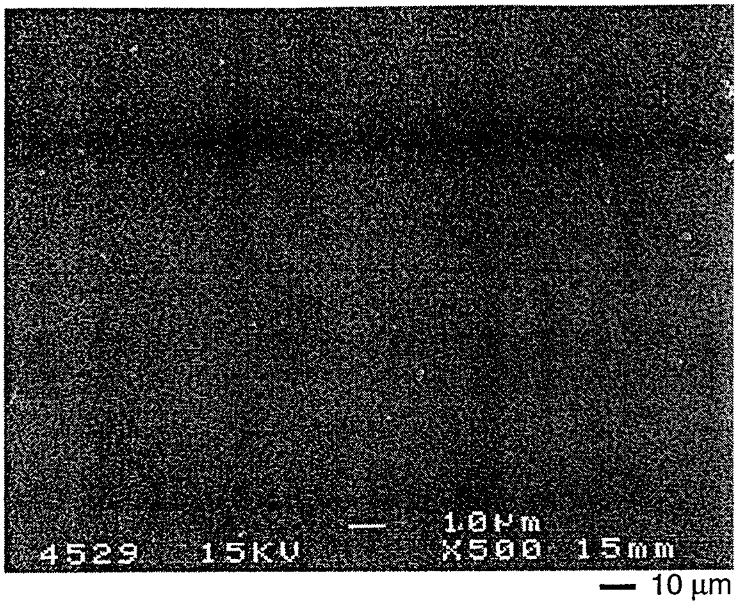

Figure 2a

Secondary electron image showing the absence of porosity in the Ce SYNROC. (500x)

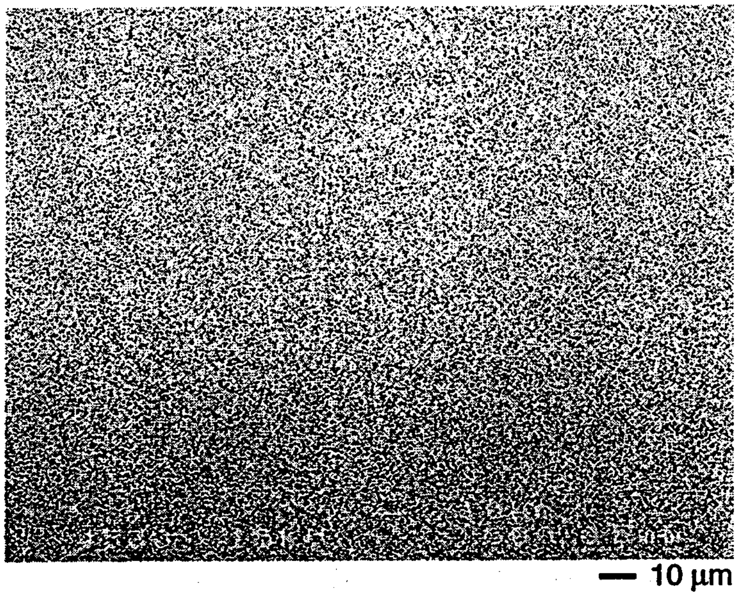

Figure 2b

Backscattered electron image showing homogeneity of the Ce SYNROC. (500x)

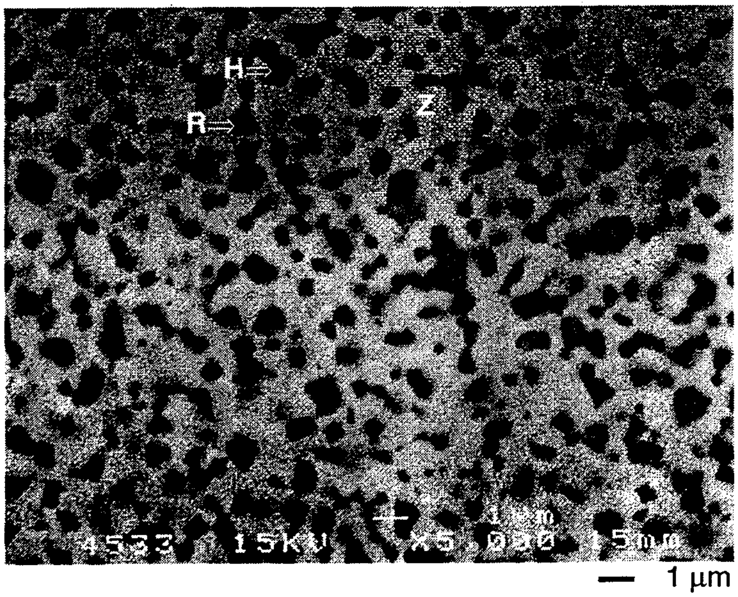

Figure 2c

Backscattered electron image showing detail of the phases present in the Ce SYNROC. (5000x) Z = Zirconolite, H = Hollandite, R = Rutile

FIGURE 2 : SEM Images of the Ce SYNROC Material HIPed at 1270°C.

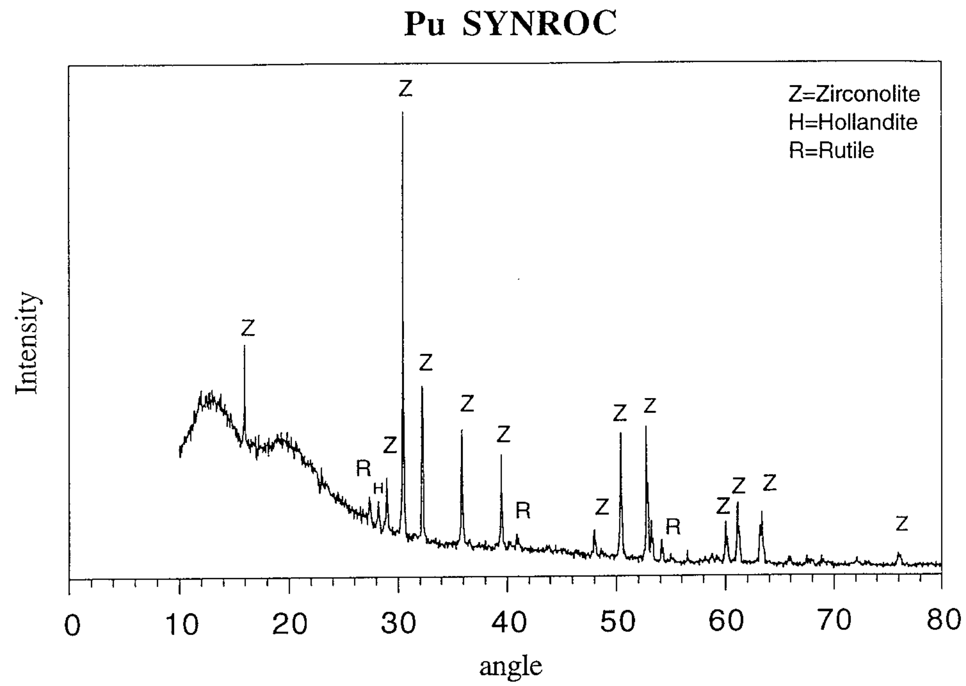
Pu SYNROC

(a) Pu bearing SYNROC Material : X-ray diffraction data (Cu Kα radiation).

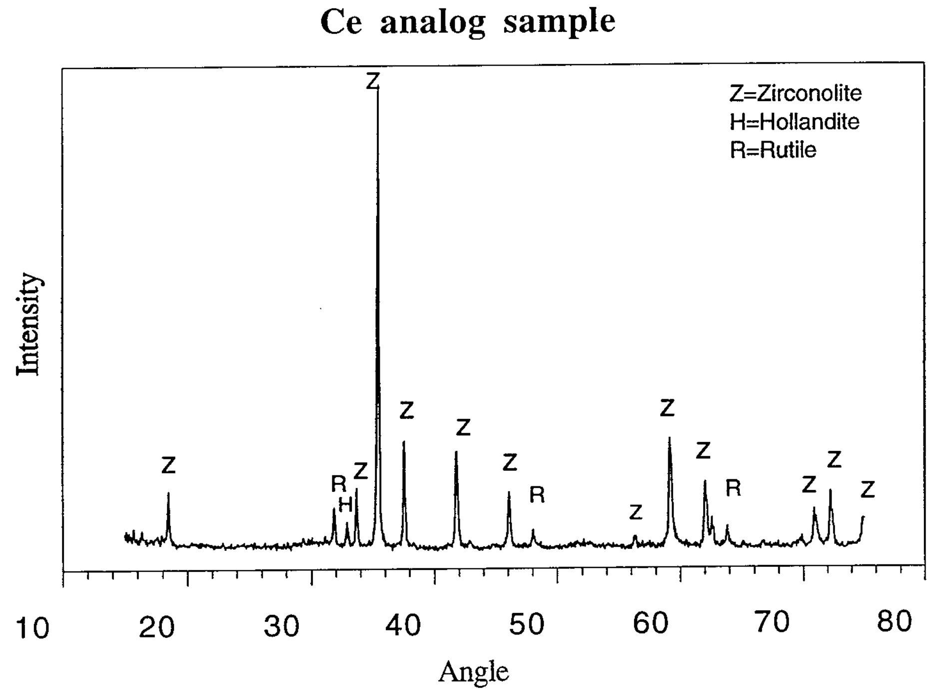
Ce analog sample

(b) Ce analog sample : X-ray diffraction data (Co Kα radiation).

FIGURE 3 : X-ray Diffraction Data for Material from HIP cans.

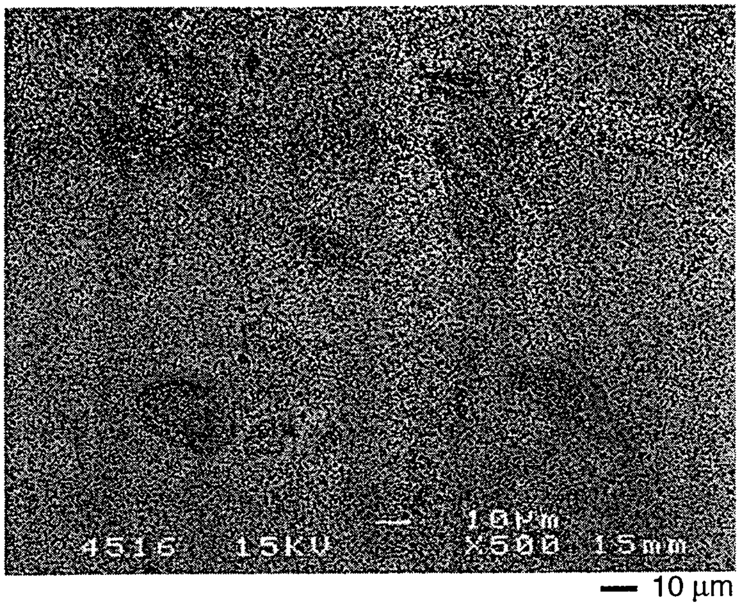

Figure 4a

Low magnification backscattered electron image of the Ce SYNROC from the large HIP can. (500x)

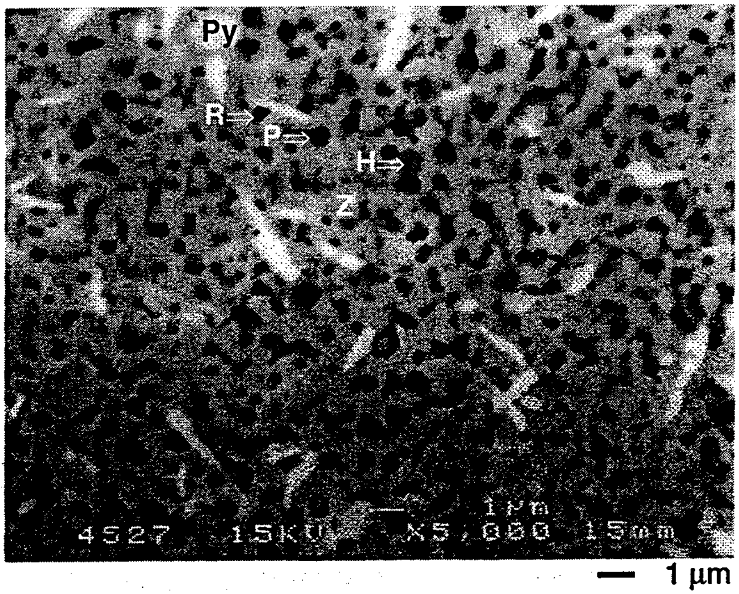

Figure 4b

Backscattered electron image showing fine grained Ce SYNROC with some Pyrochlore present. (5000x). Z = Zirconolite, H = Hollandite, R = Rutile, P = Pores, Py = Pyrochlore.

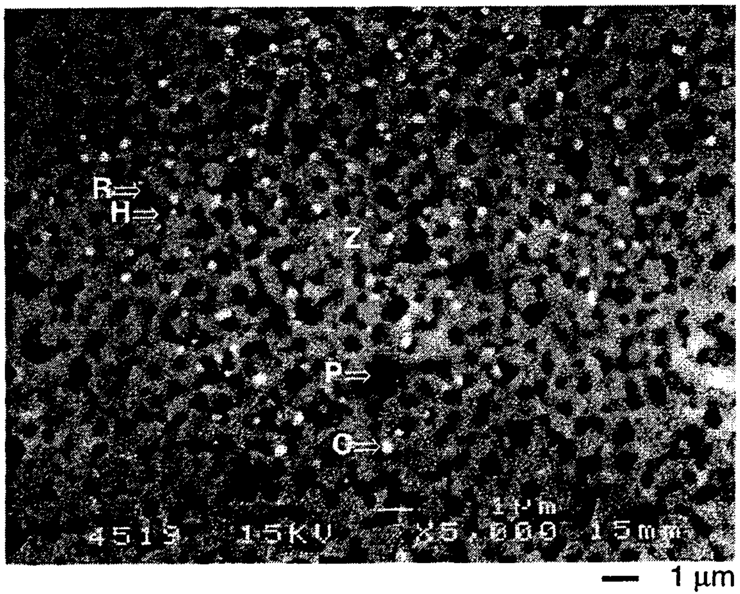

Figure 4c

Backscattered electron image showing fine grained Ce SYNROC with some CeO_2 possibly present (the small size of these particles made them difficult to analyse). (5000x). Z = Zirconolite, H = Hollandite, R = Rutile, P = Pores, C = possible CeO_2.

FIGURE 4 : SEM Images Showing the Types of Microstructure found in the large (10Kg) can of Ce SYNROC Material, HIPed at 1240°C.

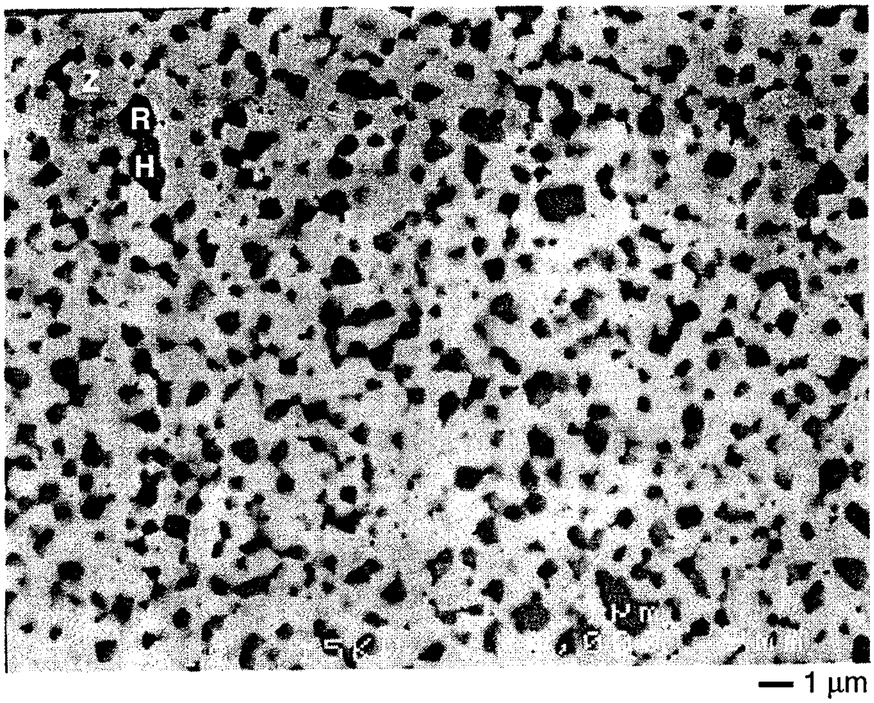

Figure 5a: Backscattered electron image of Ce SYNROC HIPed at 1270°C, and then re-heated to 1100°C and cooled at 0.5 °C/min to 900°C before furnace cooling to ambient temperatures. (4000x)

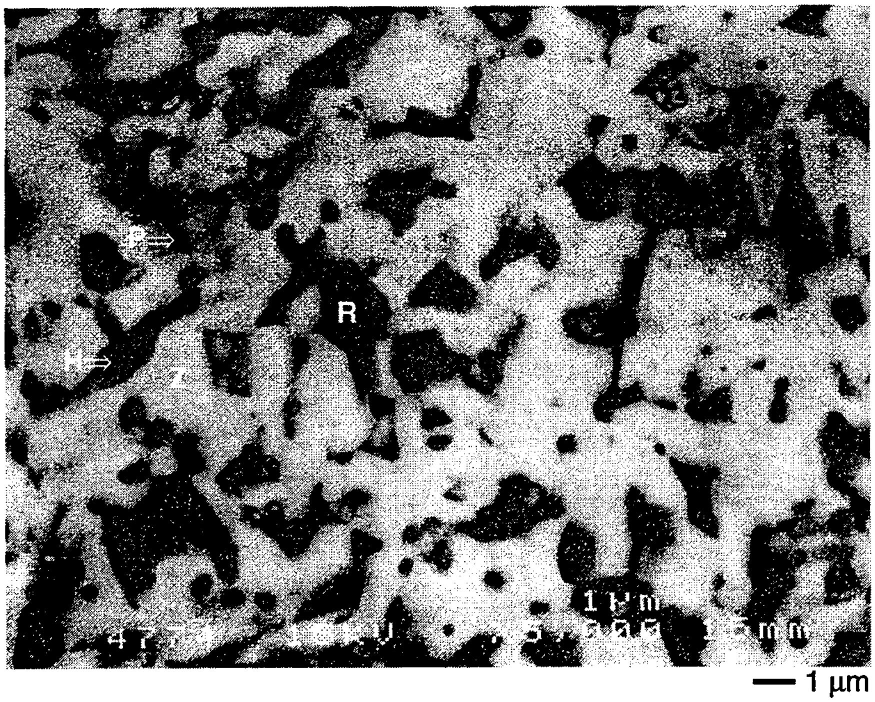

Figure 5b: Backscattered electron image of Pu SYNROC HIPed at 1280°C, and then re-heated to 1100°C and cooled at 0.5 °C/min to 900°C before furnace cooling to ambient temperatures. (5000x)

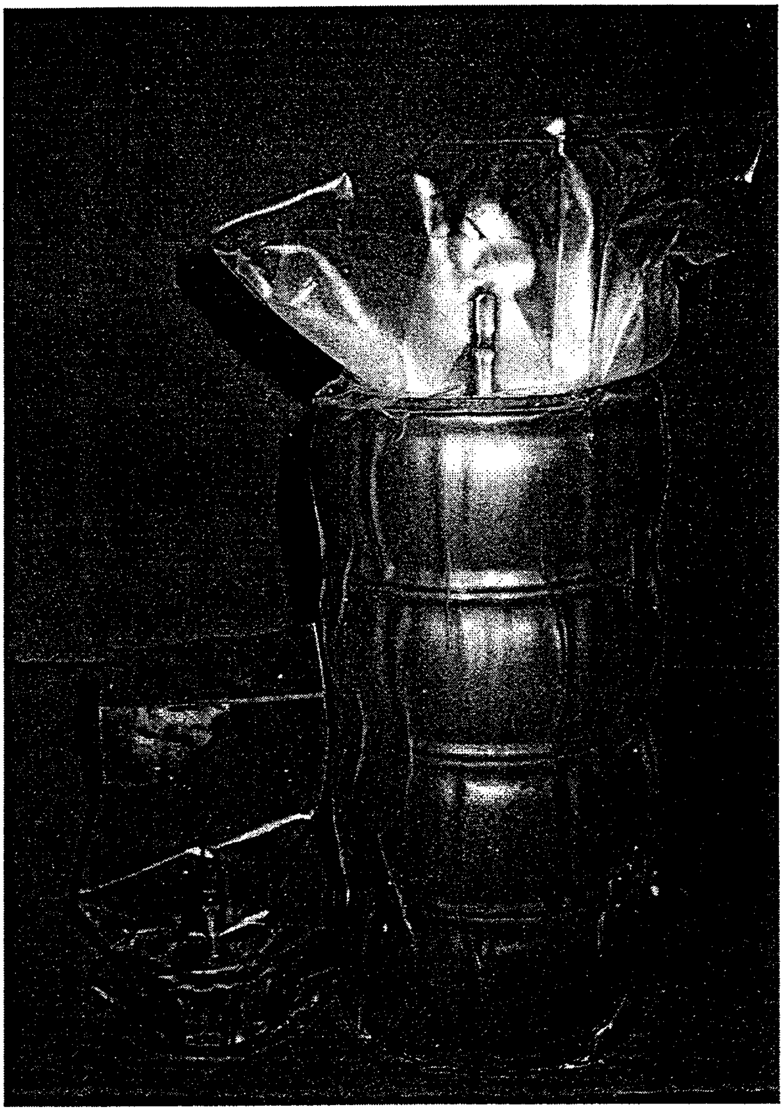

Figure 6 : HIPed cans of zirconolite-rich SYNROC, containing CeO_2 as simulant for PuO_2, prior to shipment to LLNL (items 2 and 3).

Figure 7 : HIPed can of zirconolite-rich SYNROC containing 50g of PuO_2 (item1).

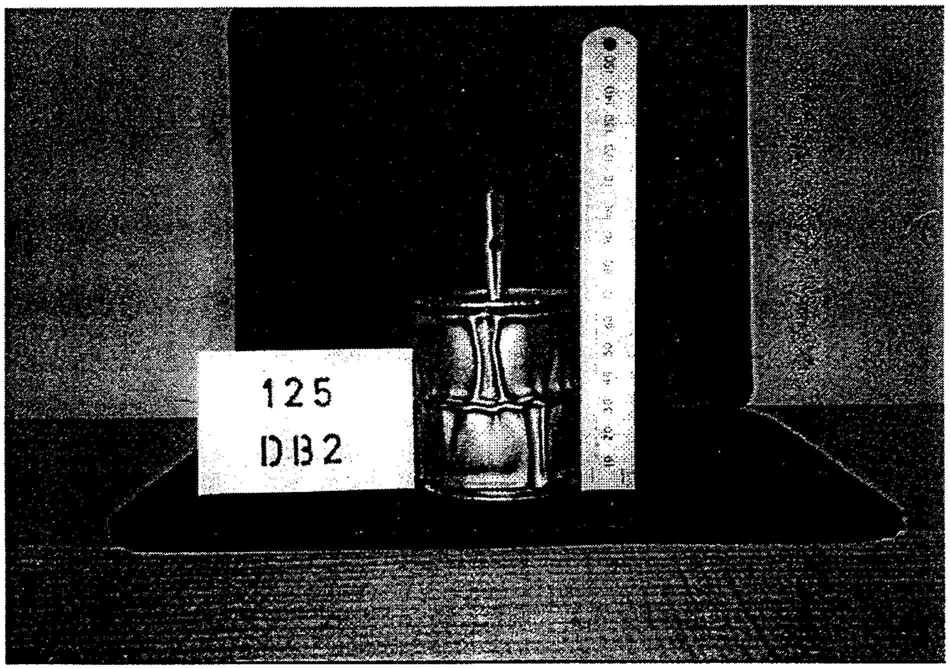

Figure 8 : HIPed can of CeO_2 substituted zirconolite-rich SYNROC. This can provides additional material to that in item 2 (Fig. 6) for independent characterisation.